
NUCLEAR EXPERIMENTAL
TECHNIQUES

Dark Currents of a Tandem Accelerator with Vacuum Insulation

V. I. Aleinik, A. A. Ivanov, A. S. Kuznetsov,
I. N. Sorokin, and S. Yu. Taskaev

*Budker Institute of Nuclear Physics, Siberian Branch, Russian Academy of Sciences,
pr. Akademika Lavrent'eva 11, Novosibirsk, 630090 Russia*

Received August 6, 2012

Abstract—The dark currents flowing in the high-voltage gaps of an electrostatic tandem accelerator with vacuum insulation and the effects associated with their occurrence are investigated. This accelerator, featuring a fast rate of charged particle acceleration and a large surface area of the accelerating electrodes, has been designed to produce a proton beam with an energy of 2 MeV and a constant current of up to 10 mA.

DOI: 10.1134/S002044121304012X

An electrostatic tandem accelerator with vacuum insulation—a new type of accelerator capable of generating a proton beam with an energy of 2 MeV and a constant current of up to 10 mA has been designed and put into operation [1, 2]. The issues of optimizing high-voltage ageing of the accelerator in the cases of its complete and partial breakdowns were considered in [3]. In this paper, the results of the high-voltage accelerator tests allowing identification of the dark currents flowing in the high-voltage gaps were analyzed.

The design of the tandem accelerator with vacuum insulation is shown in Fig. 1. Injected negative oxygen ions are accelerated to an energy of 1 MeV by the potential applied to the high-voltage electrode and converted into protons in the gaseous stripping target; afterward, the protons are accelerated in the same field to 2 MeV. The gas is pumped out of the stripping target by the cryogenic and turbomolecular (TMP_1 – TMP_3) pumps via a louver system located at the top of the high-voltage electrodes—shields. The potential is supplied to the high-voltage electrode and five transfer electrodes from the high-voltage source via a feedthrough insulator with a resistive voltage divider mounted in it.

This accelerator is characterized by a high electric field strength in the interelectrode gap (~ 25 kV/cm) and a large total area of the electrodes (tens of square meters). The vacuum was in the range of 10^{-3} – 10^{-5} Pa when the accelerator was held at a high voltage in the beamless operating mode.

According to [4–6], dark currents having different origins will inevitably flow in the interelectrode gaps of such a system. Since the active voltage divider is used on the insulator to set the potentials of the electrodes—shields and the current in this divider is low (several hundreds of microamperes), the dark currents in the accelerating gaps are capable of exerting a significant

effect on the potential distribution along the accelerating channel and, therefore, on beam transportation, focusing, and acceleration. As a result, the necessity arises to study the dark currents in the accelerating gaps.

DIAGNOSTIC TOOLS

The high-voltage electrode potential is measured by means of two resistive voltage dividers of the high-voltage power supply and the feedthrough insulator. From now on, the signals from the reference resistors of these dividers will be called “the voltage of the power supply divider” and “the voltage of the insulator divider,” respectively. In the absence of the currents in the interelectrode spaces, these voltages are identical.

In the presence of the dark currents, the voltage of the insulator divider may differ from the accelerator voltage, since the potentials of the transfer electrodes are specified by the divider in the feedthrough insulator. The lower voltage of the insulator divider is the indication that the predominant dark current is in the gap between the vacuum tank and the first accelerating electrode, and the higher voltage is the evidence that the predominant dark current flows in the space between the accelerating electrodes.

The dark current in the gap between the vacuum tank and the first accelerating electrode is determined from the difference in the current of the high-voltage supply and the current in the feedthrough insulator divider. The dark current in the other accelerating gaps can be calculated, assuming that it is uniform, from the difference of the accelerator voltage from the insulator divider voltage.

The vacuum is measured by a Pfeiffer Vacuum PKR 251 compact vacuum lamp having a linear sensitivity for air over a wide pressure range. It is

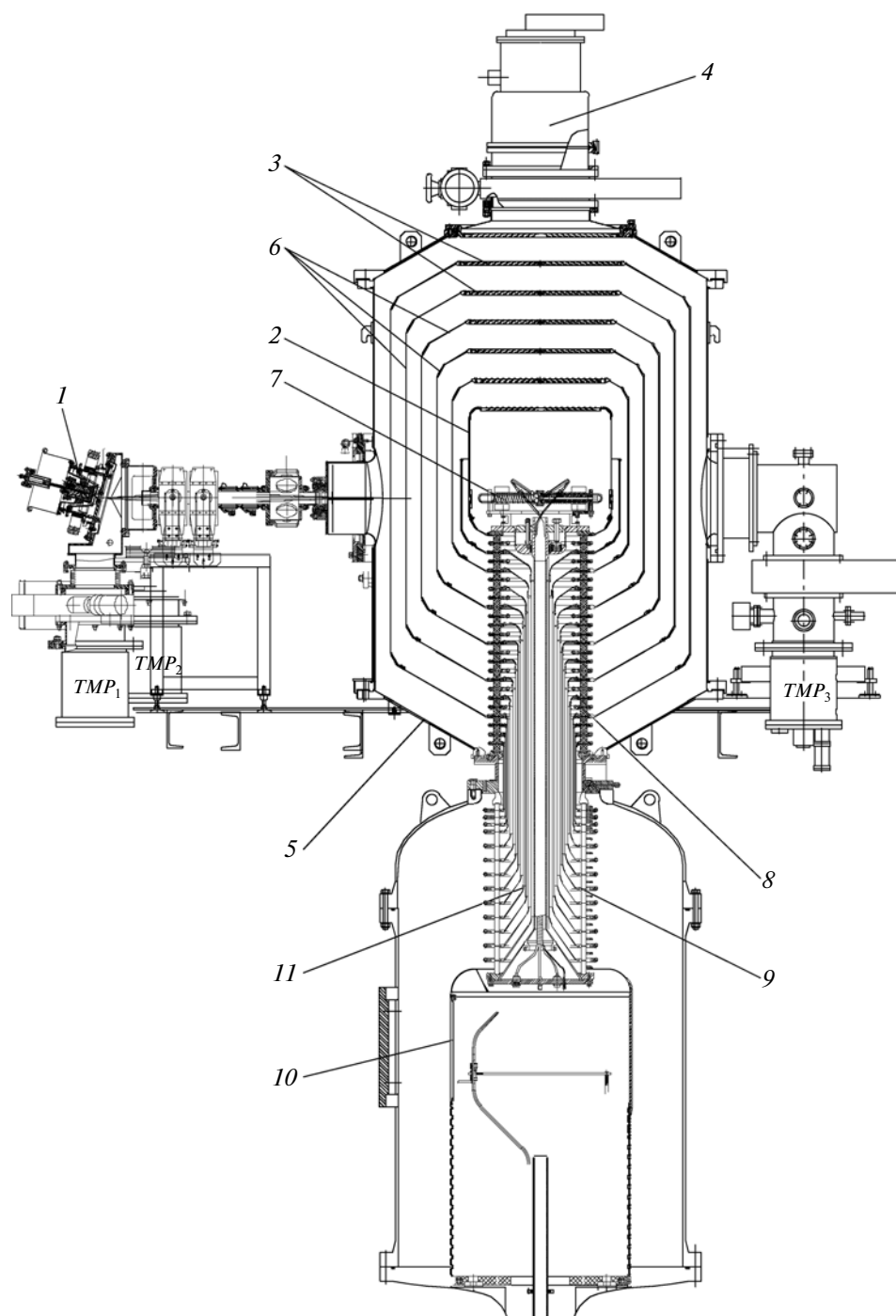


Fig. 1. Tandem accelerator with vacuum insulation: (1) source of negative hydrogen ions, (2) high-voltage electrode, (3) louvers of the electrodes—shields, (4) cryogenic pump, (5) vacuum tank of the accelerator, (6) transfer electrodes—shields of the accelerator, (7) gaseous charge-exchange target, (8) vacuum part of the high-voltage insulator, (9) gas part of the high-voltage insulator, (10) high-voltage source, and (11) internal coaxial cylinders that connect the equipotential electrodes of the gas and vacuum insulator parts.

installed immediately at the accelerator output in the pumping-down elbow of turbomolecular pump TMP_3 (Fig. 1). The ionizing radiation dose rate is measured by the automatic radiation monitoring system, which was described in detail in [7].

DARK CURRENT DETECTION

Ageing of the accelerator implies a smooth increase in the voltage and, thereafter, holding the instrument for several hours at the operating voltage. A stable effect is observed at an increased voltage (Fig. 2): the

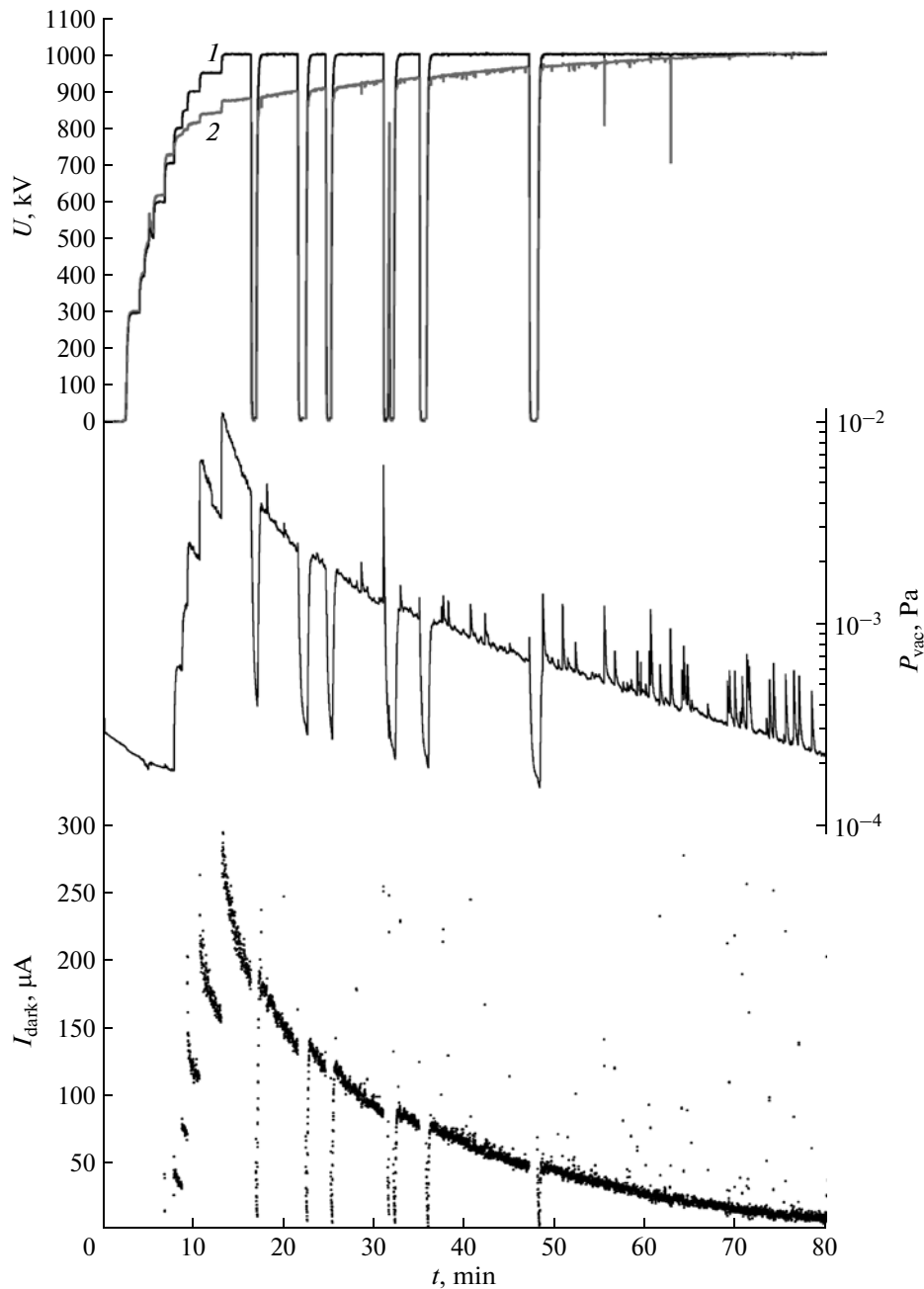


Fig. 2. Ageing curves.

voltage readings of the insulator divider ($U_{d\ ins}$, curve 2) lag behind the voltage readings of the power supply divider ($U_{d\ sup}$, curve 1). This effect can be explained by the appearance of dark currents in the accelerating gaps, which are caused by generation of microdischarges followed by desorption of adsorbed gases from the electrode surfaces when the voltage goes up.

According to [4], microdischarges result from mutual secondary emission of positive and negative ions and are followed by intense gas release; therefore, an increase in the pressure in the vacuum volume is

observed when the electrode area is large. Stopping of the voltage rise results in a slow suppression of desorption, which can increase again upon further increase in the voltage.

The time dependences of the residual gas pressure P_{vac} in the vacuum volume and dark current I_{dark} in the accelerating gap between the wall of the vacuum tank and the adjacent accelerating electrode corroborate the above explanation. After the current protection of the high-voltage rectifier operates, the voltage is removed

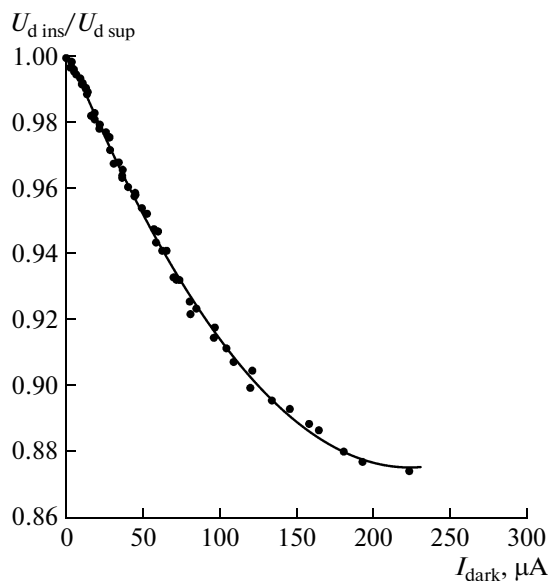


Fig. 3. Dependence of the $U_{d \text{ ins}}/U_{d \text{ sup}}$ ratio on the dark current in the first gap.

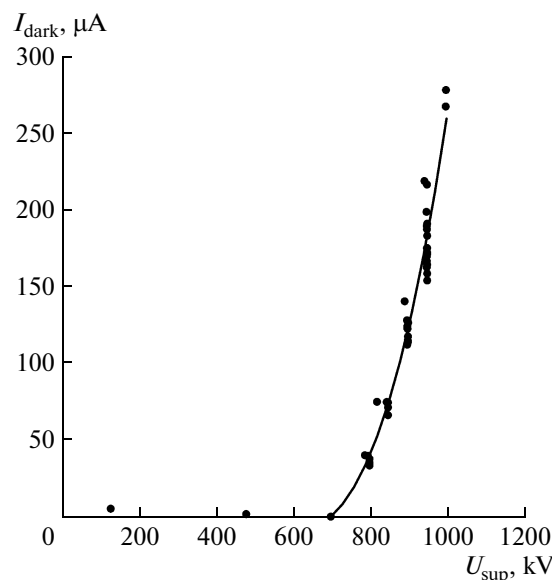


Fig. 4. Experimental dependence of the dark currents in the accelerating gaps of the accelerator on the supply voltage.

from the accelerator. It is apparent that, at these instants of time, the residual pressure is improved.

The characteristic positive surges of the residual pressure can be attributed to breakdowns most of which are partial and do not trigger the current protection. In Fig. 2, it is apparent that, upon holding under tension, the vacuum is improved, the current in the accelerating gap decreases, and the difference in the divider voltages practically disappears in ~ 1 h.

Figure 3 presents ratio $U_{d \text{ ins}}/U_{d \text{ sup}}$ versus the dark current, referred from Fig. 2 for a supply voltage of 1 MV. The voltage ratio values are averaged over five experiments with a spread in the values within $\pm 5\%$ relative to the mean. The dark current values also differ only slightly within the limits of each experimental point $U_{d \text{ ins}}/U_{d \text{ sup}}$. It is apparent that there is an unambiguous dependence of the ratio of these voltages on the dark current value, which highlights their interrelationship.

The nonlinear dependence of the load current (I_{load}) of the voltage source on $U_{d \text{ sup}}$ corresponded to nonlinear dependence $U_{d \text{ ins}}/U_{d \text{ sup}}$ on $U_{d \text{ sup}}$ in the experiment. The difference between the load current of the voltage source and the sum of the currents from all resistive dividers ($I_{\text{dark}} = I_{\text{load}} - \Sigma I_d$) of the accelerator as a function of the supply voltage is shown in Fig. 4 by a solid line with experimental dots. The appearance of the additional current in the accelerator's vacuum volume coincides in the voltage with the onset of vacuum deterioration.

To estimate these currents, let us use the schematic diagram of the voltage dividers of the high-voltage source, which simulate the occurrence of the conduc-

tivity of the vacuum insulation for the accelerating gaps (Fig. 5).

The divider of the powerful voltage source resides in a tank filled with sulfur hexafluoride, inside the secondary loop of the rectifier in the homogeneous field. One end of the divider is connected to the high-voltage electrode of the source, and the other end is connected to the "ground" electrode. The intermediate points of the divider connection with the setup components are absent.

The insulator divider is kept in sulfur hexafluoride. The divider components are fixed in positions on the electrodes of both the vacuum and gas parts of the feedthrough insulator. The main function of the divider is to specify the potentials applied to the electrodes of the accelerating gaps. All divider resistors labeled in the diagram consist of a set of resistors connected in series and in parallel.

The resistors of the insulator divider are connected to the electrodes of the vacuum accelerating gaps at points $A-G$ so that the high-voltage electrode corresponds to point A and the "ground" electrode corresponds to point G . Numeration of the electrodes and accelerating gaps starts with the ground electrode. In the absence of the uncontrollable currents in the high-voltage gaps, the readings of the supply and insulator dividers must coincide.

Resistors r_4-r_9 simulate the appearance of the conductivity and, hence, of the dark currents between the accelerating electrodes. In the absence of the dark currents, $r_4-r_8 \rightarrow \infty$. From the diagram, it is apparent that the value of the current flowing through resistor r_9 can be determined as the difference between the volt-

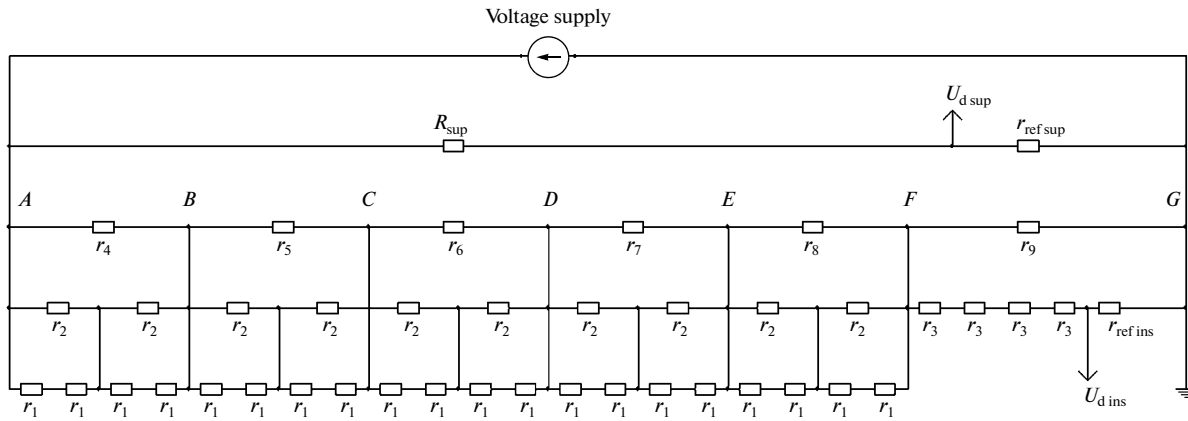


Fig. 5. Circuit diagram of the active voltage dividers of the high-voltage supply and the feedthrough insulator: (r_1) divider resistors for the vacuum part of the insulator, (r_2, r_3) divider resistors for the gas part of the insulator, ($r_{ref ins}$) reference resistor of the insulator divider, ($R_{sup}, r_{ref sup}$) arms of the high-voltage supply divider, and ($U_{d ins}, U_{d sup}$) signals from the dividers of the insulator and the high-voltage supply, multiplied by the appropriate voltage ratios.

age supply load current and the total current of all resistive dividers. It is this method for determining the current by the first accelerating gap that has been used in the experiment.

If the current occurs only in the first gap or this current exceeds the other currents, ratio $U_{d ins}/U_{d sup}$ decreases and, at the same time, the voltage across each of the remaining five accelerating gaps grows in

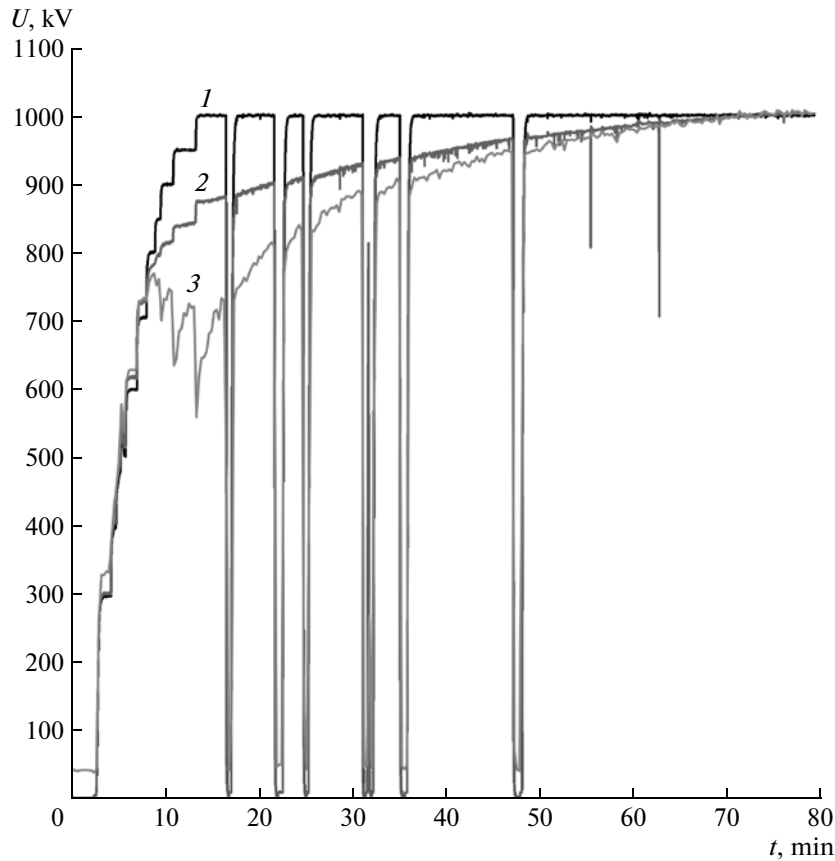


Fig. 6. Dependence of the voltage applied to the dividers (1) of the source and (2) of the insulator, and (3) theoretical curve for the insulator voltage in the presence of the dark currents only in the first gap.

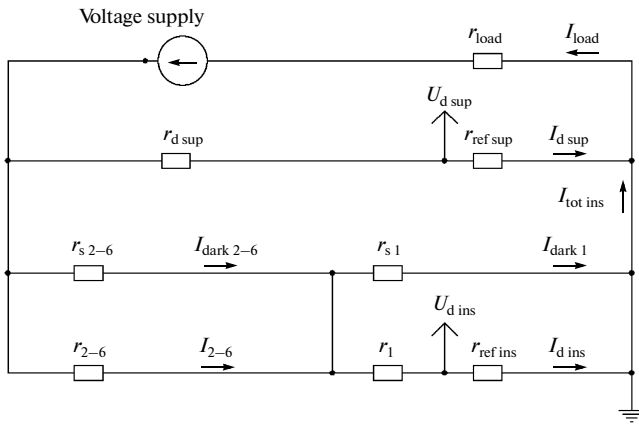


Fig. 7. Simplified diagram of the voltage dividers for the high-voltage source and the feedthrough insulator.

value. The current of the insulator divider increases in the same proportion, which must be taken into account when selecting the power of the used resistors. If the currents in each of the five gaps exceed the current in the first accelerating gap, the readings of the insulator divider will exceed the readings of the supply divider.

If other dark currents except for the dark current detected in the first gap are absent in the system, the voltage of the insulator divider is calculated in accordance with the diagram by the formula

$$U_{d \text{ ins}} = U_{\text{sup}} - \left(\frac{20r_1 r_2}{2r_1 + r_2} \right) I_{r_1}$$

The experimentally determined voltages $U_{d \text{ ins}}$ differ from the values calculated by this formula (Fig. 6), which points to the impossibility of explaining the observed difference in the readings of the insulator divider and the high-voltage supply divider by the presence of the dark current in the first accelerating gap only.

To calculate the dark currents, let us take into account the following fact: the size of the louvers through the slits of which the gas is mostly pumped out of the inner volume of the accelerator; the geometry of the electrodes in all accelerating gaps, except for the first; and the operating electric field strength in all the gaps differ only slightly. Therefore, the dark currents of a discharge in each of the five gaps also must not substantially differ.

The geometry of the first gap differs from the others by the presence of the holes in the ground electrode, intended for injection and extraction of the ion beam, and the hole for the cryogenic exhaust pump. The diameters of all holes in the ground electrode exceed significantly the value of the first gap, and the electric field in the region of these holes exceeds the fields of the “smooth” coaxial electrodes of the other high-

voltage gaps, thus increasing the probability that additional currents will occur.

The dark currents in the five accelerating gaps were evaluated using a simplified circuit diagram of the voltage dividers of the high-voltage source and the feedthrough insulator (Fig. 7), which was equivalent to the diagram presented in Fig. 5. The calculation was performed under the assumption that the currents in these five gaps were equal.

The total current through the first accelerating gap and the voltage divider segment corresponding to this gap is $I_{\text{tot ins}} = I_{\text{dark1}} + I_{d \text{ ins}}$, and the voltage across the first gap is $U_1 = I_{\text{dark}} r_{s1} = I_{d \text{ ins}} (r_1 + r_{\text{ref ins}})$. Therefore, the total voltage across the five gaps and the corresponding segments of the insulator divider is $U_{2-6} = U_{\text{sup}} - U_1$, and the dark current in five vacuum gaps can

$$\text{be written as } I_{\text{dark2-6}} = I_{\text{tot ins}} - \frac{U_{2-6}}{r_{2-6}}.$$

The results of calculations performed for one of the experiments are presented in Fig. 8. It is apparent that, at the beginning of the experiment, the current value averaged over five gaps $I_{\text{dark2-6}}$ is smaller than the dark current measured in the first gap. In the course of the experiment $I_{\text{dark2-6}}$ decreases to the minimum value at a higher rate than the dark current in the first gap. This can be explained by the surface quality of the ground electrode, which differs from that of the other electrodes (the tank surface is polished, and the electrode surfaces are mirror-finished), as well as by the features of its geometry, such as the presence of the hole for the cryogenic pump and the holes with a larger radius relative to the other electrodes for beam injection and extraction.

The occurrence of the current load in the gaps causes the voltage to be redistributed among the gaps and increases the probability of accelerator breakdown. At the stage when the accelerator was brought to the full voltage, an experiment was conducted with the aim of determining the mean time between breakdowns at different residual pressures and a full voltage of 1 MV. Each cycle of measurements included observation of five breakdowns in one range of residual pressures and five breakdowns in the other range. These cycles were repeated three times. As the residual pressure increased, the time between breakdowns decreased. In this case, the relevant vacuum gaps and structural components connected in parallel to them (insulation rings and gas gaps, see Fig. 1) were overloaded in the voltage by 4% or less due to the gas discharge current in the first gap.

MICROBREAKDOWN DETECTION

The oscilloscope traces of the signals in the process of smooth voltage rise are presented in Fig. 9. It is apparent that, at a voltage of >400 kV, microbreak-

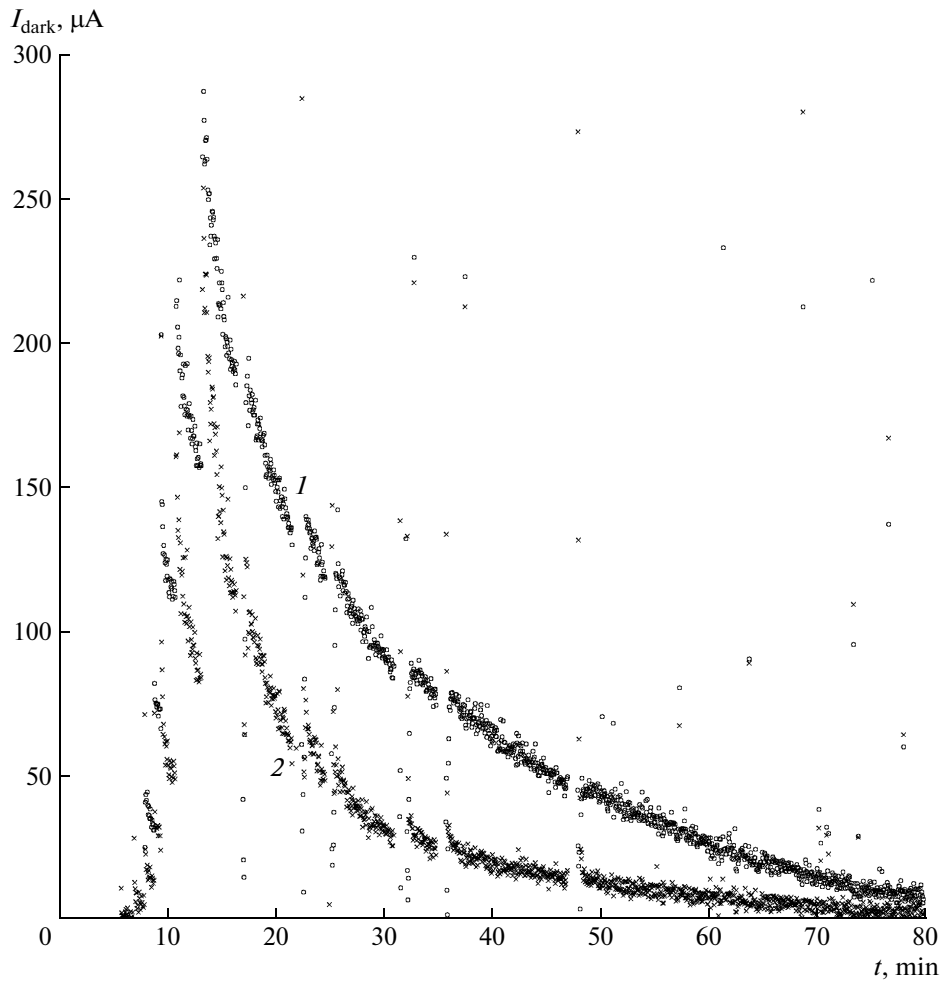


Fig. 8. Change in the dark current (I) of the first gap in the course of the experiment and (2) theoretical curve of the current in the other five gaps.

downs happen in the gaps between the accelerating electrodes. Since the voltage of the insulator divider increases sharply upon a breakdown, this indicates that the current in the gaps between the accelerating electrodes is predominant. At the same time, the dark current always flow in the first accelerating gap upon each microbreakdown (Fig. 9b).

Each microbreakdown is followed by gas desorption, which is clearly distinguishable on the pressure curves (Fig. 9c) and radiation bursts (Fig. 9d). It should also be noted that, at voltages of >700 kV, the dark current changes from the pulsed to the stationary mode. The figure demonstrates one more interesting effect: since time instant $t = 610$ s, a sharp decrease in the X-ray dose rate upon deterioration of the vacuum conditions has been observed.

HIGH-INTENSITY DARK CURRENT

In a set of experiments aimed at increasing the beam current in the beamline of negative hydrogen

ions, the diameters of the electrode holes were increased from 20 to 58 mm, except for the high-voltage electrode in which the hole diameter remained unchanged (20 mm). After this change, frequent occurrence of the high-intensity dark current has been detected: as early as after the accelerator ageing, when the dark current decreased to the characteristic values of several tens of microamperes, it suddenly increased to 3–4 mA [8].

For example, in one of the experiments, a dark current of 3.2 ± 0.5 mA was flowing for 100 s in the first accelerating gap. Since the voltage of the insulator divider was by 18% higher than the accelerator voltage, the dark current between the electrodes was, according to the calculations, by $100 \mu\text{A}$ higher than the dark current from the ground. In comparison with the standard ageing mode, flowing of such a current caused a twofold increase in the gas release and almost hundredfold increase in the radiation dose rate.

The latter fact is the evidence of a higher electron energy, which is possible when, instead of flowing

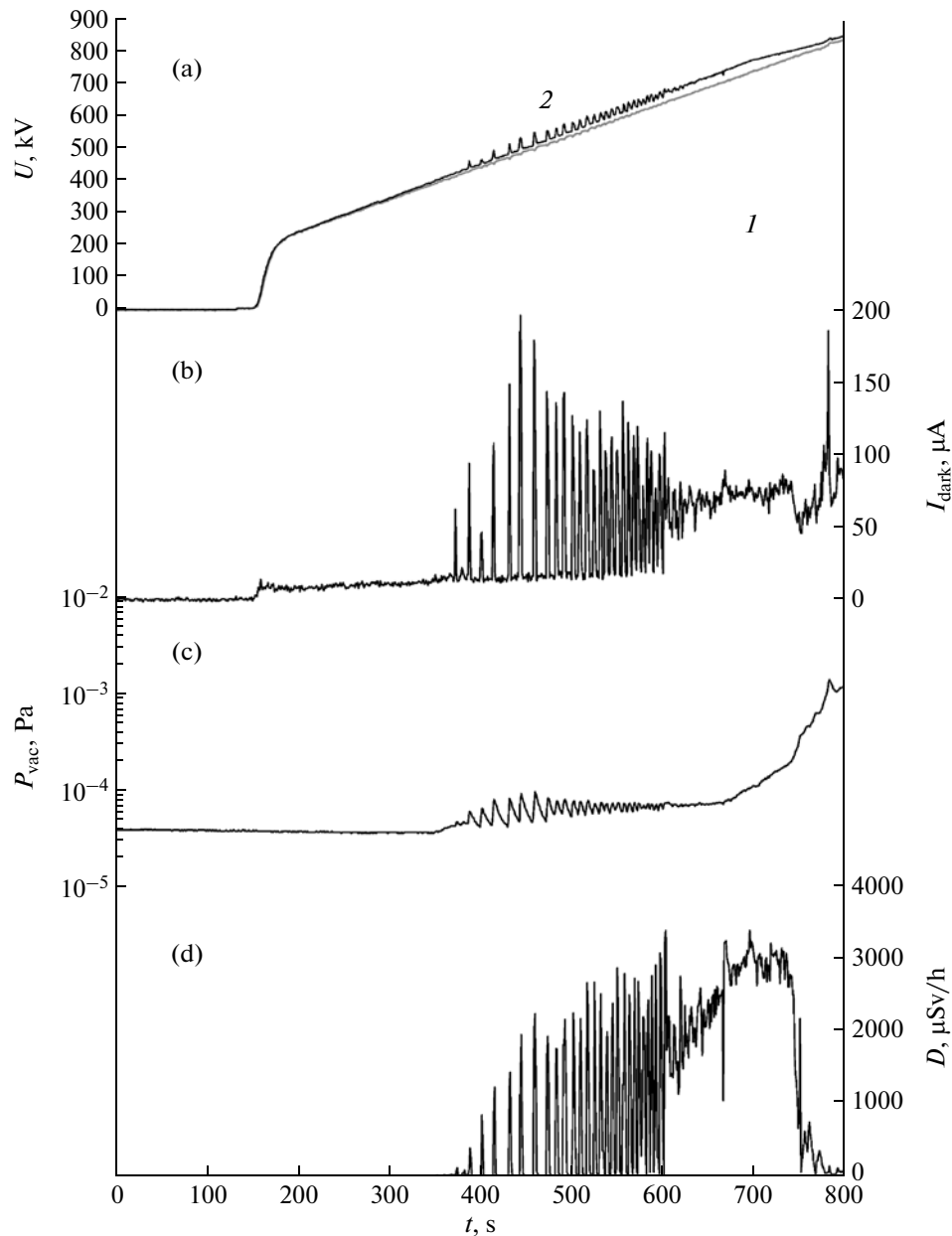


Fig. 9. Time dependences (a) of the voltages applied (1) to the accelerator and (2) to the insulator divider, (b) dark current, (c) vacuum pressure, and (d) X-ray dose rate.

between the adjacent electrodes, the current in the gap flows, e.g., between the vacuum tank casing or the first electrode and the high-voltage electrode. This assumption was confirmed by measuring the X-ray spectrum using a scintillation BGO spectrometer [9]. The peak in the spectrum was shifted from 120 to 400 keV. In [9], it has also been shown that a significant increase in the X-ray dose rate can be attributed not only to an increase in the energy yield of the bremsstrahlung due to the increase in the electron energy, but also to the significantly weaker attenuation of X rays by the 6-mm-thick steel walls of the vacuum tank.

After opening of the accelerator's vacuum chamber, a part of the high-voltage electrode diaphragm appeared to melt. The numerical calculation of the electrostatic fields has shown that, when the beamline aperture increases, the electric field strength at the sharp edge of the hole in the cathode part of the diaphragm fastening frame increases from 42 to 51 kV/cm, which may result in an intense emission of electrons, which are carried immediately into the acceleration channel. To prevent the occurrence of this current, the channel aperture was reduced, and the sharp edges of the diaphragm fastening frame were rounded.

CONCLUSIONS

The results of tests of the high-voltage accelerator components were analyzed. This analysis provided a means for identifying the dark currents flowing in the high-voltage gaps. The method for evaluating the value of the dark current was described and the observed phenomena associated with its flow were explained.

ACKNOWLEDGMENTS

This work was supported by the Ministry of Education and Science of the Russian Federation, state contract nos. 16.518.11.7038 and 14.518.11.7039.

REFERENCES

1. Bayanov, B.F., Belov, V.P., Bender, E.D., et al., *Nucl. Instrum. Methods Phys. Res., A*, 1998, vol. 413, p. 397.
2. Kuznetsov, A.S., Malyshev, G.N., Makarov, A.N., Sorokin, I.N., Sulyaev, Yu.S., and Taskaev, S.Yu., *Tech. Phys. Lett.*, 2009, vol. 35, no. 8, p. 346.
3. Sorokin, I.N. and Shirokov, V.V., *Instrum. Exper. Tech.*, 2007, vol. 50, no. 6, p. 719.
4. Slivkov, I.N., Mikhailov, V.I., Sidorov, V.I., and Nas-tyukha, A.I., *Elektricheskii proboi i razryad v vakuume* (Electrical Discharge and Breakdown in Vacuum), Moscow: Atomizdat, 1966.
5. Slivkov, I.N., *Elektroizolyatsiya i razryad v vakuume* (Electric Insulation and Discharge in Vacuum), Moscow: Atomizdat, 1972.
6. Espe, V., *Tekhnologiya elektrovakuumnykh materialov* (Technology of Electrovacuum Materials), Moscow: Gosenergoizdat, 1962.
7. Barkova, V.G., Koryabkin, O.M., Repkov, A.V., and Chudaev, V.Ya., Automated system of radiation control of VEPP-4 electron-positron accelerated-accumulative complex, *Trudy devyatogo Vsesoyuznogo soveshchaniya po uskoritelyam zaryazhennykh chastits* (Proc. 9th All-Union Meeting on Charged Particle Accelerators), Dubna: OIYaI, 1985, vol. 2, p. 318.
8. Aleinik, V.I., Kuznetsov, A.S., Sorokin, I.N., et al., *Preprint of Budker Inst. of Nucl. Phys.*, Novosibirsk, 2012, no. 2012-2.
9. Bashkirtsev, A.G., Ivanov, A.A., Kasatov, D.A., et al., *Med. Fizika*, 2012, no. 2, p. 5.

Translated by N. Goryacheva